Title: Intrinsic regulators of the action potential waveform control dopamine release to shape behavior

One sentence summary: We show that ion channels in midbrain dopamine neurons are critical for patterning neurotransmitter release to regulate reinforcement learning.

Authors: Barbara Juarez[1,2], Mi-Seon Kong[1], Yong S. Jo[1,§], Jordan E. Elum[1], Joshua X. Yee[1], Scott Ng-Evans[1], Marcella Cline[1], Avery C. Hunker[2,†], Madison A. Baird[2,‡], Meagan A. Quinlan[1], Adriana Mendez[1%], Nastacia L. Goodwin[3], Marta E. Soden[2], Larry S. Zweifel*[1, 2].

Affiliations:

[1]Department of Psychiatry and Behavioral Sciences, University of Washington; Seattle, WA, United States.

[2] Department of Pharmacology, University of Washington; Seattle, WA, United States.

[3] Department of Biostructure, University of Washington; Seattle, WA, United States.

§ Current affiliation: School of Psychology, Korea University; Seoul, Republic of Korea.

†Current affiliation: Allen Brain Institute; Seattle, WA, United States.

‡ Current affiliation: Cajal Neuroscience; Seattle, WA, United States

% Current affiliation: National Institute on Alcohol Abuse and Alcoholism;Rockville, MD, United States

*Corresponding author. Email: larryz@uw.edu

Abstract:

Despite the widely known role of dopamine in reinforcement learning, how the patterns of dopamine release that are critical to the acquisition, performance, and extinction of conditioned responses are generated is poorly resolved. Here, we demonstrate that the coordinated actions of two ion channels, Kv4.3 and BKCa1.1, control the pattern of dopamine release on different time scales to regulate separate phases of reinforced behavior in mice. Inactivation of Kv4.3 in VTA dopamine neurons increases pacemaker activity and excitability that is associated with increased ramping prior to lever press in a learned instrumental response paradigm. Loss of Kv4.3 enhanced performance of the learned response and facilitated extinction. In contrast, loss of BKCa1.1 increased burst firing and phasic dopamine release that enhanced learning of an instrumental response. Inactivation of BKCa1.1 increased the reward prediction error that was associated with an enhanced extinction burst in early extinction training. These data demonstrate that temporally distinct patterns of dopamine release are regulated by the intrinsic properties of the cell to shape behavior.

Introduction

Reinforcement learning is an essential process by which an organism links environmental stimuli and actions with outcomes. Dopamine-producing neurons in the ventral tegmental area (VTA) of the midbrain facilitate reinforcement learning to promote the performance of goal-oriented behavior through modulation of information processing in the forebrain, most notably in the nucleus accumbens (NAc) (*1*). Distinct patterns of dopamine release that occur on different time scales during the acquisition, performance, and extinction of a conditioned response are thought to underlie dopamine function within these contexts (*2-5*). Despite the evidence that dopamine is critical for reinforcement learning (*1-3*), how the intrinsic properties of the cell contribute to dopamine release, and whether patterns of release observed during learning and subsequent performance of a conditioned response influence patterns of release during extinction is not well resolved. Moreover, recent findings suggest that dopamine release dynamics can occur independently of the activity patterns at the cell body (*5*) raising the possibility that the firing properties of dopamine neurons may be dispensable for some aspects of reinforcement learning.

VTA dopamine neurons display spontaneous action potential firing in the absence of afferent inputs (*6*) that is regulated by a suite of voltage-gated ion channels (*7-9*). Potassium currents shape the action potential waveform to regulate the frequency and pattern of firing (*7-10*). Kv4.3 subunits contribute to A-type potassium currents (I_A) in dopamine neurons (*8*) that facilitate repolarization and control the frequency of firing (*8*). BKCa1.1 subunits are the essential subunit of voltage-sensitive, calcium-activated big conductance potassium. (BK) channels conduct BK currents (I_{BK}) that mediate the initial phase of the action potential afterhyperpolarization to control the pattern of firing (*9*). To determine whether these intrinsic regulators of dopamine neuron action potential firing influence neurotransmitter release dynamics and reinforcement learning, we

targeted the inactivation of two potassium channel subunit encoding genes in these cells, Kv4.3 (gene name: *Kcnd3*) and BKCa1.1 (gene name: *Kcnma1*) using CRISPR/Cas9 mutagenesis. We found that inactivation of Kv4.3 and BKCa1.1 differentially affected the action potential waveform, neuronal excitability, and patterns of action potential firing. We further show that loss of function (LOF) of these two channels differentially impacted the acquisition, maintenance, and extinction of a reinforced behavioral response that was associated with distinct effects on the patterns of dopamine release during these behaviors. Specifically, loss of BKCa1.1 enhanced burst firing and phasic dopamine release that was associated with enhanced acquisition of instrumental behavior and a heightened extinction burst. In contrast, loss of Kv4.3 increased dopamine neuron excitability, elevated ramping of dopamine release prior to a lever press in a learned instrumental reinforcement task, and facilitated extinction. These findings demonstrate that intrinsic regulators of the action potential waveform influence dopamine release dynamics that control the patterns of behavior during reinforcement learning.

Results

CRISPR/Cas9 inactivation of Kv4.3 and BKCa1.1

To determine the distribution of *Kcnd3* and *Kcnma1* expression in the VTA, we performed RNAscope *in situ* hybridization to quantify the mRNA levels for these ion channel subunits and the rate-limiting enzyme in dopamine production, *Th*. We find that Kv4.3 and BKCa1.1 subunits are expressed in most dopamine neurons along the rostral-caudal axis (Fig. 1, A-C, fig. S1, A-E), suggesting that these ion channels regulate the activity of the majority of these cells. To selectively inactivate these two channels, we used a viral-mediated, Cre-inducible CRISPR/SaCas9 system (*11*). Adeno-associated viruses (AAV) containing single guide RNA directed to either of the two loci (AAV1-FLEX-SaCas9-sg*Kcnd3* or AAV1-FLEX-SaCas9-sg*Kcnma1*) were generated (Fig. 1,

D and H) and injected into the VTA of separate groups of adult *Slc6a3*(DAT)-IRES-Cre mice (fig. S2, A; fig. S3-S4). This yielded high efficiency indel formation and loss of function (LOF) for both channel subunits in dopamine neurons relative to controls (Fig.1, E-G, I-K; fig. S2 B-C; fig. S4, A-C). Specifically, AAV1-FLEX-SaCas9-sg*Kcnd3* nearly abolished the AmmTx-sensitive A-type potassium conductance (Fig. 1, F and G) and AAV1-FLEX-SaCas9-sg*Kcnma1* significantly reduced the iberiotoxin-sensitive BK conductance (Fig. 1, J and K; fig. S4, A-C).

Kv4.3 and BKCa1.1 regulation of dopamine neuron activity

As predicted, Kv4.3 LOF altered the dopamine neuron action potential waveform by increasing the action potential half width and slowing repolarization relative to control and BKCa1.1 LOF cells (Fig. 2, A-D, control mice). BKCa1.1 LOF reduced afterhyperpolarization relative to control and Kv4.3 cells and resulted in a more depolarized resting membrane potential relative to control cells (Fig. 2, A-B, E-F). Neither manipulation affected the peak of the action potential (fig. S4, D). Kv4.3 LOF increased excitability (Fig. 2, G-H) and frequency of spontaneous action potential firing relative to control cells (Fig. 2 I-J). BKCa1.1 LOF did not affect these parameters (Fig. 2 G-J) but shifted the pacemaker-like *ex vivo* activity observed in control and Kv4.3 LOF cells to a more irregular pattern, as evidenced by an increase in the coefficient of variation in the interspike interval (CV-ISI) (Fig. 2, I and K; fig. S4, E).

Increased CV-ISI in VTA dopamine neurons of BKCa1.1 LOF mice is consistent with a shift to more burst-like activity (*10*); however, this pattern of firing by dopamine neurons is most accurately assessed by recording neural activity *in vivo*. Using optical isolation (*12*) to identify dopamine neurons during *in vivo* recording (fig. S5, A-C), we found that BKCa1.1 LOF increases the number of spikes in a burst and burst duration of VTA dopamine neurons relative to controls (Fig. 2, L-M), with no effects on baseline firing rate or the frequency of burst events (fig. S5, D-

E). Kv4.3 LOF did not alter *in vivo* firing properties under these basal conditions (Fig. 2, L-M; fig. S5, D-E).

Kv4.3 and BKCa1.1 differentially regulate instrumental behavior and dopamine release

To assess whether LOF of these ion channels impacts reinforcement learning, we first trained Kv4.3 and BKCa1.1 LOF mice in an appetitive Pavlovian conditioning paradigm where a lever extension followed by retraction (CS) signals reward (Rew) delivery (fig S6). We did not observe differences between Kv4.3 LOF and BKCa1.1 LOF mice relative to controls (fig. S6, A-C) indicating that dopamine regulation by these channels is not essential for this simple form of learning. Next, mice were transitioned to a fixed-ratio (FR1) schedule of operant reinforcement learning in which lever retraction and reward delivery were contingent on a lever press (LP). Extension of the lever that had previously served as the onset of the CS was now contingent on reward retrieval by making a head entry (HE) into the food hopper (Fig. 3, A); thus, serving as a conditioned reinforcer (CR). BKCa1.1 LOF learned the task faster than control and Kv4.3 LOF mice, as evidenced by a higher frequency of lever presses in the first half of the session on day 1 of conditioning in BKCa1.1 mice (Fig. 3, B-C; fig. S6, D-F). Kv4.3 LOF and control mice increased responding between the first and second day that remained elevated on the third day; however, Kv4.3 LOF mice now earned more rewards on the third day of conditioning than BKCa1.1 LOF mice (Fig. 3, B) and had a higher frequency of responding in the first half of the session on day 3 (Fig. 3, D; fig. S6, G-I), a flip of what was observed on day 1 of conditioning. Differences in reinforcement learning were not associated with changes in overall locomotor activity (fig. S7, A-B) and did not reflect changes in motivation (fig. S7, C). These findings indicate that BKCa1.1 LOF enhances acquisition of the learned response, but Kv4.3 LOF enhances performance once the task is learned.

To determine how these ion channels contribute to dopamine release dynamics during the distinct phases of reinforcement learning, we expressed the genetically encoded dopamine sensor dLight1.3b (*13*) in the NAc of Kv4.3 LOF, BKCa1.1 LOF, and control mice (fig. S8) and performed fiber photometry during FR1. Mice underwent Pavlovian conditioning followed by the transition to FR1 instrumental conditioning as described above. Due to the restrictive nature of the tethering for fiber photometry recording, mice underwent 5 days of FR1 instead of 3 days and dopamine signals were measured on day 1 and day 5. Control mice showed phasic increases in dopamine time-locked to LP, Rew, and HE/CR on day 1 (Fig. 3, E top row) and day 5 (Fig. 3, E middle row, bottom row). Kv4.3 LOF mice showed highly variable LP and Rew dopamine signals on the first day and HE/CR signals are undetectable (Fig. 3, F top row); clear signals to these events emerged on day 5 (Fig. 3, F middle row, bottom row). BKCa1.1 LOF mice had significantly larger dopamine release events to LP, Rew, and HE/CR on day 1 (Fig. 3, G-H). Dopamine release was decreased on day 5 relative to day 1, except in Kv4.3 LOF mice though the pattern of release is largely consistent (Fig. 3, E-J). Kv4.3 LOF mice displayed a significantly higher peak in the ramp of dopamine release just prior to the lever press on day 5 of conditioning relative to control mice (Fig. 3, K). Cumulative summation (CuSum) analysis of the ramp period revealed that although the ramp was higher in Kv4.3 LOF mice, the start of the ramp, or inflection point, was not different (Fig. 3, L). These data demonstrate that these ion channels regulate the patterns of dopamine release differentially during the acquisition of conditioned response and during performance of the response once it is learned.

Kv4.3 and BKCa1.1 in dopamine neurons differentially influence extinction

Following Pavlovian and FR1 conditioning, a subset of mice underwent extinction training with reward omission (Fig. 4, A). Control mice exhibited an extinction burst in lever pressing on

the first day of extinction (higher pressing on day 1 of extinction versus the last day of reinforced FR1 conditioning). This extinction burst is elevated in BKCa1.1 LOF mice relative to control mice (Fig. 4, B; fig. S9, A-C). In contrast, Kv4.3 LOF mice had significantly reduced lever presses during the first day of extinction training relative to both control and BKCa1.1 LOF mice (Fig. 4, B; fig. S9, A-C). The number of lever presses in BKCa1.1 LOF and control mice decreased during the extinction session but remained relatively stable in Kv4.3 LOF mice (Fig. 4, C; fig S9. A-B). All mice performed similarly on the last day of extinction (Fig. 4, B; fig. S9, D-F). Interestingly, lever pressing on the first day of extinction was proportional to the level of responding on the first day of FR1 conditioning (fig. S9, G), suggesting that enhanced acquisition is associated with an invigorated response when the outcome (reward omission) does not match expectation (reward).

During extinction training, dopamine signals were largely undetectable to the lever press on the first and last day of extinction training (fig. S9, H-I). In contrast, control mice had a small phasic dopamine response immediately following HE/CR (period A) that quickly returned to baseline (period B) and was further reduced on the fifth day of extinction (Fig. 4, D-F). Kv4.3 LOF mice had a small, but detectable phasic dopamine response during period A that was followed by a sustained signal during period B (Fig. 4, D-F; Wilcoxon sign rank test relative to zero, $P<0.05$). BKCa1.1 LOF mice did not display a phasic increase to the HE/CR period A on either day, but had a significant reduction in the dopamine signal during period B (Fig. 4, D-F), consistent with an enhanced reward prediction error (*14*).

Discussion

Our results confirm that viral-mediated CRISPR/Cas9 mutagenesis is an effective means to study ion channel function in the central nervous system of adult mice. Using this strategy, we showed that Kv4.3 and BKCa1.1 differentially contribute to the action potential waveform and the

174 pattern of action potential firing. We found that altering the firing properties of dopamine neurons
175 to increase pacemaker activity or to induce irregularity and enhance burst firing had differential
176 effects on behavior and dopamine release. These findings support the conclusion that the intrinsic
177 electrophysiological properties of VTA dopamine neurons that contribute to the action potential
178 waveform are critical to the regulation of the neurotransmitter release dynamics that govern
179 behavior.

180 Slowing the action potential repolarization through inactivation of Kv4.3 increased the
181 frequency of action potential firing and excitability. The exact mechanism(s) that underlie Kv4.3
182 regulation of excitability and pacemaker activity are not clear. The most obvious explanation is
183 the contribution of A-type potassium current to the negative feedback during rapid depolarization
184 (*8*). Another potential mechanism is the observation that decreasing Kv4.3 in cardiomyocytes
185 increases sodium conductance (*15*); thus, Kv4.3 LOF may enhance subthreshold sodium currents
186 previously shown to regulate pacemaker activity in VTA dopamine neurons (*16*).

187 Increased ramping of dopamine release prior to lever press observed in Kv4.3 LOF mice
188 following instrumental learning is likely a reflection of an increased activity of VTA dopamine
189 neurons associated with descending GABAergic disinhibitory mechanisms (*17*). Through the
190 regulation of membrane repolarization (*8*) and in the absence of this inhibitory influence, ramping
191 is elevated that enhances performance of the learned response, consistent with previous assertions
192 on the function of ramping (*3-5*). In contrast to previous reports that ramping of dopamine release
193 occurs independently of the activity at the cell body (*5*), our data demonstrate that the intrinsic
194 excitability of the cell, regulated by Kv4.3, contributes to this process.

195 As predicted, BKCa1.1 reduced the action potential afterhyperpolarization (*9*). We did not
196 observe effects of reduced BK current on the action potential width or an increase in pacemaker

activity as reported in substantia nigra pars compacta (SNc) dopamine neurons (*9*), suggesting that BK currents regulate firing in distinct ways in these two dopaminergic regions. Consistent with previous reports of decreasing the action potential afterhyperpolarization (*18, 19*), we find that inactivation of BKCa1.1 increased spile irregularity *ex vivo* and burst firing *in vivo*. In the absence of BKCa1.1 channels burst events are prolonged which enhances phasic dopamine release. Based on previous findings (*2, 3, 14, 20, 21*), this elevation in phasic dopamine would be predicted to assign a higher value to action and the outcome to facilitate the acquisition of the instrumental response and enhance the reward prediction error (*2, 3, 14, 20, 21*). In contrast to BKCa1.1 LOF, during early extinction, Kv4.3 LOF promoted a small but sustained activation. We propose that this lack of a prediction error prevents the behavioral extinction burst and facilitates the cessation of responding.

We focused on Kv4.3 and BKCa1.1 in dopamine neurons because of their selective and enrichment and their ubiquitous expression across VTA dopamine neurons. It is important to note that these channels are expressed widely throughout the brain where they likely serve similar functions in patterning transmitter release. Further, numerous other ion channels contribute to the action potential. The emergence of many of these ion channels as hotspots of missense mutations in neurodevelopmental disorders (*22*) reinforces the importance of understanding how these channels influence cellular and systems function.

References

1. R. A. Wise, Dopamine, learning and motivation. *Nat Rev Neurosci* **5**, 483-494 (2004).
2. W. Schultz, Multiple dopamine functions at different time courses. *Annu Rev Neurosci* **30**, 259-288 (2007).
3. H. R. Kim *et al.*, A Unified Framework for Dopamine Signals across Timescales. *Cell* **183**, 1600-1616 e1625 (2020).
4. M. W. Howe, P. L. Tierney, S. G. Sandberg, P. E. Phillips, A. M. Graybiel, Prolonged dopamine signalling in striatum signals proximity and value of distant rewards. *Nature* **500**, 575-579 (2013).
5. A. Mohebi *et al.*, Dissociable dopamine dynamics for learning and motivation. *Nature* **570**, 65-70 (2019).
6. S. W. Johnson, R. A. North, Two types of neurone in the rat ventral tegmental area and their synaptic inputs. *J Physiol* **450**, 455-468 (1992).
7. M. Marinelli, C. N. Rudick, X. T. Hu, F. J. White, Excitability of dopamine neurons: modulation and physiological consequences. *CNS Neurol Disord Drug Targets* **5**, 79-97 (2006).
8. Z. M. Khaliq, B. P. Bean, Dynamic, nonlinear feedback regulation of slow pacemaking by A-type potassium current in ventral tegmental area neurons. *J Neurosci* **28**, 10905-10917 (2008).
9. T. Kimm, Z. M. Khaliq, B. P. Bean, Differential Regulation of Action Potential Shape and Burst-Frequency Firing by BK and Kv2 Channels in Substantia Nigra Dopaminergic Neurons. *J Neurosci* **35**, 16404-16417 (2015).
10. M. E. Soden *et al.*, Disruption of dopamine neuron activity pattern regulation through selective expression of a human KCNN3 mutation. *Neuron* **80**, 997-1009 (2013).
11. A. C. Hunker *et al.*, Conditional Single Vector CRISPR/SaCas9 Viruses for Efficient Mutagenesis in the Adult Mouse Nervous System. *Cell Rep* **30**, 4303-4316 e4306 (2020).
12. S. Q. Lima, T. Hromadka, P. Znamenskiy, A. M. Zador, PINP: a new method of tagging neuronal populations for identification during in vivo electrophysiological recording. *PLoS One* **4**, e6099 (2009).
13. T. Patriarchi *et al.*, Ultrafast neuronal imaging of dopamine dynamics with designed genetically encoded sensors. *Science* **360**, (2018).
14. W. Schultz, P. Dayan, P. R. Montague, A neural substrate of prediction and reward. *Science* **275**, 1593-1599 (1997).
15. J. Clatot *et al.*, Inter-Regulation of Kv4.3 and Voltage-Gated Sodium Channels Underlies Predisposition to Cardiac and Neuronal Channelopathies. *Int J Mol Sci* **21**, (2020).
16. Z. M. Khaliq, B. P. Bean, Pacemaking in dopaminergic ventral tegmental area neurons: depolarizing drive from background and voltage-dependent sodium conductances. *J Neurosci* **30**, 7401-7413 (2010).
17. M. E. Soden *et al.*, Anatomic resolution of neurotransmitter-specific projections to the VTA reveals diversity of GABAergic inputs. *Nat Neurosci* **23**, 968-980 (2020).
18. P. D. Shepard, B. S. Bunney, Repetitive firing properties of putative dopamine-containing neurons in vitro: regulation by an apamin-sensitive Ca(2+)-activated K+ conductance. *Exp Brain Res* **86**, 141-150 (1991).
19. H. Ji *et al.*, Tuning the excitability of midbrain dopamine neurons by modulating the Ca2+ sensitivity of SK channels. *Eur J Neurosci* **29**, 1883-1895 (2009).

20. S. B. Flagel *et al.*, A selective role for dopamine in stimulus-reward learning. *Nature* **469**, 53-57 (2011).
21. W. Dabney *et al.*, A distributional code for value in dopamine-based reinforcement learning. *Nature* **577**, 671-675 (2020).
22. M. R. Geisheker *et al.*, Hotspots of missense mutation identify neurodevelopmental disorder genes and functional domains. *Nat Neurosci* **20**, 1043-1051 (2017).
23. B. B. Gore, M. E. Soden, L. S. Zweifel, Manipulating gene expression in projection-specific neuronal populations using combinatorial viral approaches. *Curr Protoc Neurosci* **65**, 4 35 31-20 (2013).
24. F. Wang *et al.*, RNAscope: a novel in situ RNA analysis platform for formalin-fixed, paraffin-embedded tissues. *J Mol Diagn* **14**, 22-29 (2012).
25. L. Erben, A. Buonanno, Detection and Quantification of Multiple RNA Sequences Using Emerging Ultrasensitive Fluorescent In Situ Hybridization Techniques. *Curr Protoc Neurosci* **87**, e63 (2019).
26. J. T. Ting, T. L. Daigle, Q. Chen, G. Feng, Acute brain slice methods for adult and aging animals: application of targeted patch clamp analysis and optogenetics. *Methods Mol Biol* **1183**, 221-242 (2014).
27. Y. S. Jo, G. Heymann, L. S. Zweifel, Dopamine Neurons Reflect the Uncertainty in Fear Generalization. *Neuron* **100**, 916-925 e913 (2018).

Acknowledgements: We would like to thank members of the Zweifel, Palmiter, and Chavkin laboratories at the University of Washington for their helpful discussions. We would also like to thank the staff of the University of Washington's Molecular Genetics Research Core, Comparative Medicine Animal Facilities, the University of Washington's Keck Imaging Center, and the University of Washington's Pathology Flow Cytometry Core.

Funding support: This study was supported by grants from the National Institute of Health [T32-DA727825 (B.J.), R01-DA044315 (L.S.Z.), F31-MH116549 and T32-GM007270 (A.C.H.), T32-GM007270 (M.C.), R03TR003307 (M.E.S.)] and the University of Washington's Addictions, Drugs and Alcohol Institute [ADAI-1019-17 (B.J.)]. Y.S.J. was supported in part by the National Research Foundation of Korea (MEST 2020R1A2C2102134). B.J. holds a postdoctoral Enrichment Program Award from the Burroughs Wellcome Fund. Core grants: University of Washington Keck Center [S10OD016240] and University of Washington Center of Excellence in Opioid Addiction Research NIDA [P30-DA048736].

Competing interests: The authors report no competing interests.

Author contributions: BJ and LSZ conceived and designed experiments. BJ, MES, ACH, and LZ designed and generated AAVs. BJ and MSK performed surgery. BJ and JEE performed and analyzed in situ hybridization experiments. ACH performed FACS and sequencing. BJ, MAB, AM, NLG, and MAQ performed immunohistochemical validations. BJ and MAB performed immunohistochemical quantification and analysis. BJ and MES performed in vitro electrophysiology. BJ, MK, and YSJ performed in vivo electrophysiology and analysis. BJ, JXY,

AM, and MC performed behaviors. BJ analyzed behaviors. BJ and JXY performed fiber photometry experiments. SNE generated photometry analysis software. BJ and JXY created custom MatLab code for photometry analysis. BJ and LZ further analyzed photometry data. BJ and LSZ wrote the manuscript. All authors provided input and approval of the manuscript.

List of Supplementary Materials

Materials and Methods

Fig S1 – S9

Table S1: Statistics table

Figures and legends

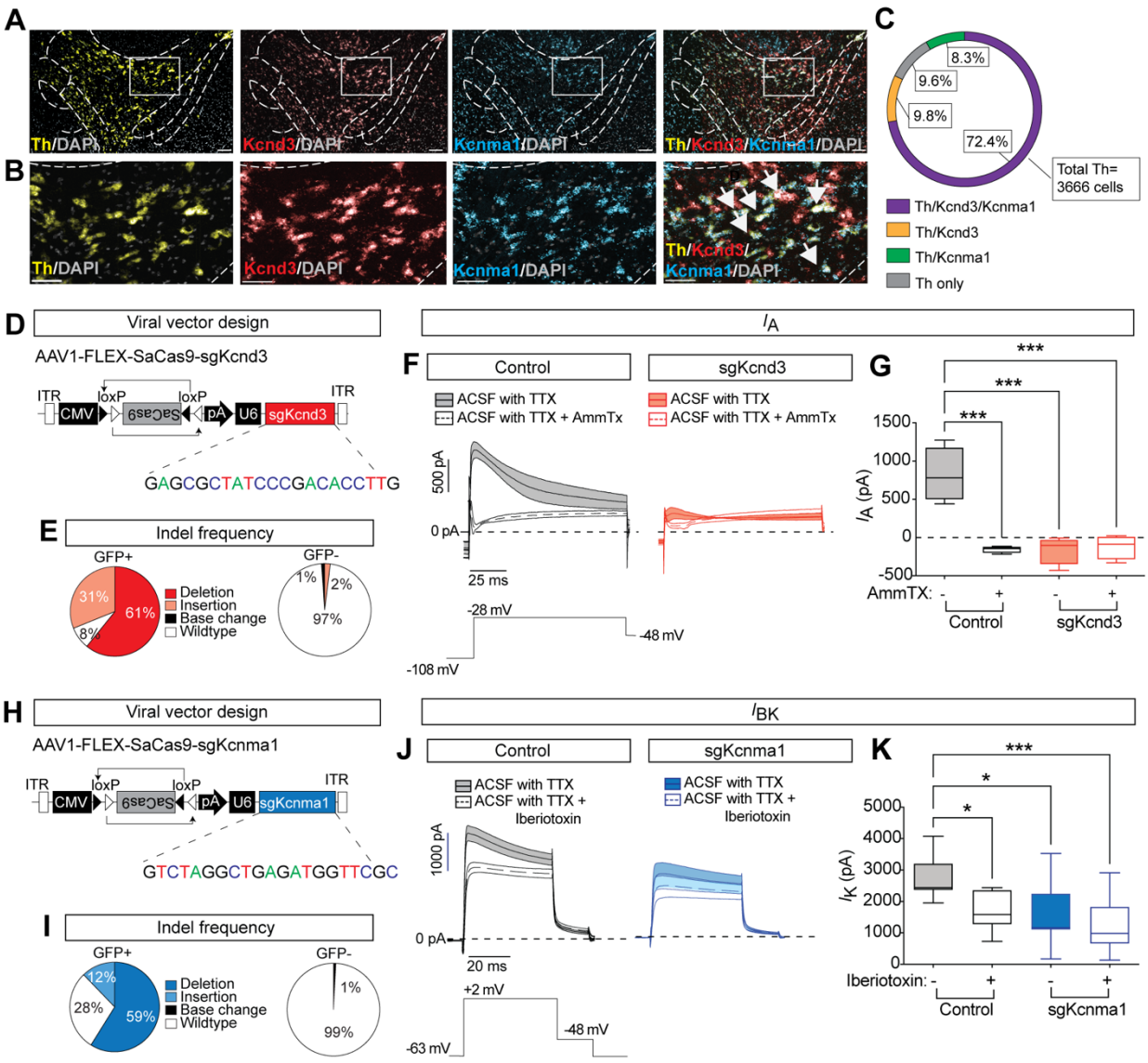

Fig. 1 Targeted mutagenesis of *Kcnd3* and *Kcnma1* in dopamine neurons.

(**A-B**) RNAscope *in situ* hybridization for *Kcnd3*, *Kcnma1*, and *Th*. White arrows: representative *Th/Kcnd3/Kcnma1* overlap. Scale bar, 100 μm (A) and 50 μm (B). (**C**) Quantification of overlap for *Kcnd3, Kcnma1,* and *Th* in the VTA (*N*=3 mice). (**D**) Schematic of AAV1-FLEX-SaCas9-sgKcnd3 targeting virus. (**E**) Proportion of targeted deep sequencing reads with indel mutations following sgKcnd3 targeting (*N*=5 mice). (**F**) Average pre- and post-AmmTx A-Type currents (I_A) from control and sgKcnd3-targeted mice (*N*=4 cells/group) and corresponding depolarization step

to elicit I_A. (**G**) Average peak I_A from (**F**) in control and sgKcnd3-targeted mice (***p<0.001). (**H**) Schematic of AAV1-FLEX-SaCas9-sgKcnma1 targeting virus. (**I**) Proportion of targeted deep sequencing reads with indel mutations following sgKcnma1 targeting (N=5 mice). (**J**) Average pre- and post-iberiotoxin (BK channel blocker) potassium currents (I_K) from control and sgKcnma1-targeted mice ($N_{control}$=11 cells; $N_{sgKcnma1}$=11 cells) and corresponding depolarization step to elicit I_K. (**K**) Peak I_K from (**J**) in control and sgKcnma1-targeted mice following iberiotoxin; notably sgKcnma1 does not have sensitivity to iberiotoxin suggesting functional loss of BK currents (*p<0.05, ***p<0.001).

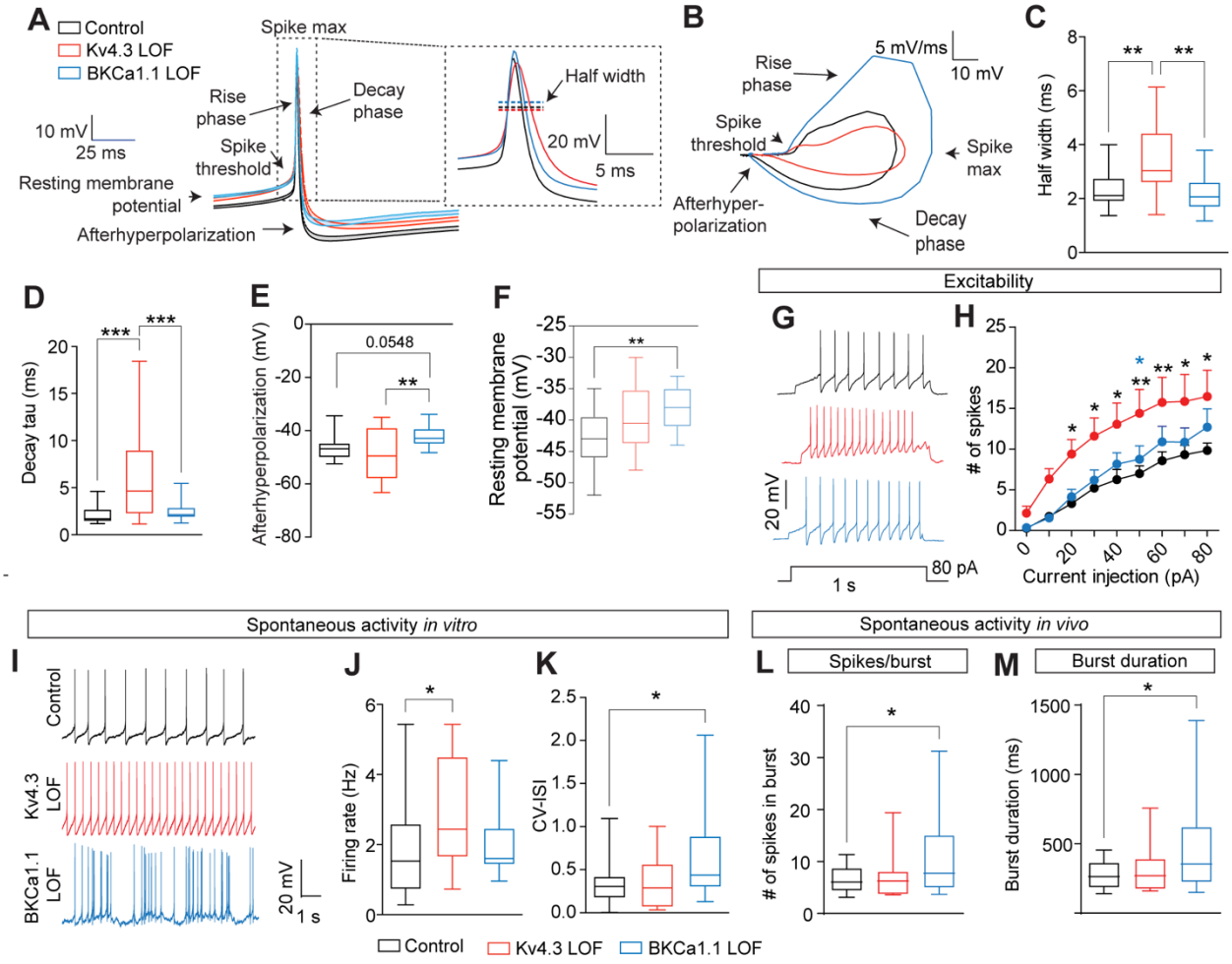

Fig. 2 Kv4.3 and BKCa1.1 LOF alter the dopamine action potential waveform and activity.

(**A**) Average action potential waveform from spontaneously active VTA dopamine neurons. (**B**) Representative phase plane plot of action potential dynamics. (**C**) Action potential half width in control, Kv4.3 LOF, and BKCa1.1 LOF cells (**p<0.01). (**D**) Decay kinetics of the action potential (***p<0.001). (**E**) Afterhyperpolarization of the action potential (**p<0.01). (**F**) Resting membrane potential (**p<0.01). (**G**) Representative evoked excitability traces. (**H**) Current-voltage plot (*p<0.05, **p<0.01: black* Kv4.3 LOF vs control, blue * Kv4.3 vs BKCa1.1 LOF; $N_{control}$=19 cells, $N_{Kv4.3\ LOF}$=15 cells, $N_{BKCa1.1LOF}$=20 cells). (**I**) Representative spontaneous activity traces. (**J**) Firing rate of spontaneous activity (*p<0.05). (**K**) CV-ISI of spontaneous activity

(*p<0.05). (**C-F** and **J-K**; $N_{control}$=21 cells, $N_{Kv4.3LOF}$=16 cells, $N_{BKCa1.1}$=19 cells). (**L**) Spikes per burst in VTA dopamine neurons *in vivo* (*p<0.05). (**M**) Burst duration in VTA dopamine neurons *in vivo* (*p<0.05). (**L-M** $N_{control}$=25 cells, $N_{Kv4.3\ LOF}$=13 cells, and $N_{BKCa1.1}$=26 cells).

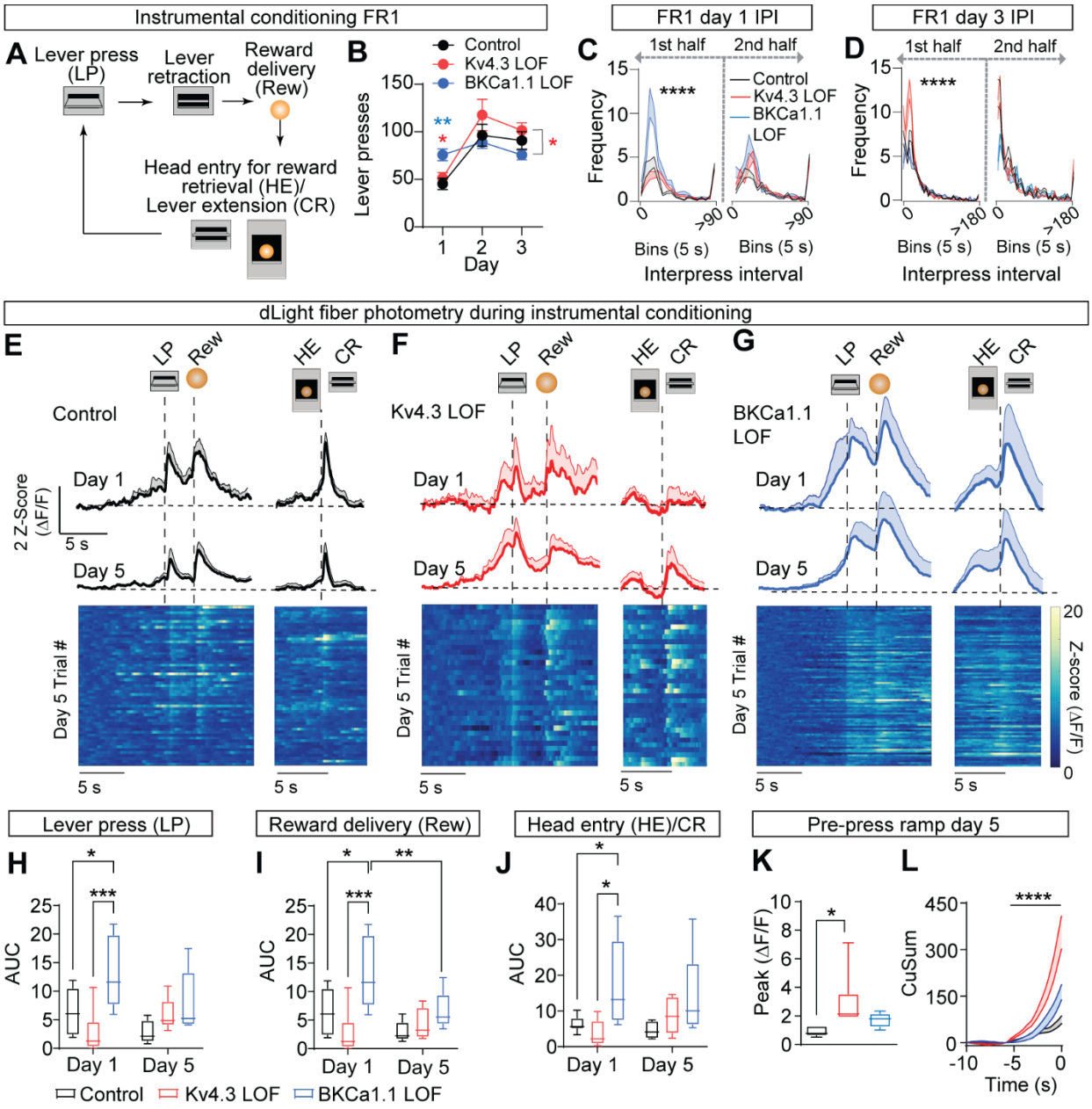

Fig. 3 Instrumental behavior and dopamine signal changes in Kv4.3 and BKCa1.1 LOF mice. **(A)** Schematic of instrumental FR1 conditioning paradigm. (**B**) Lever presses during days 1-3 of FR1 conditioning ($N_{control}$=19, $N_{Kv4.3LOF}$=24, and $N_{BKCa1.1}$=13, **p<0.01, blue=BKCa1.1 LOF vs. control; *p<0.05, red=BKCa1.1 LOF vs. Kv4.3 LOF). (**C-D**) Frequency distribution of lever inter-press intervals during the first and second half of the conditioning session for day 1 (**C**,****p<0.0001) and day 3 (**D**, ****p<0.0001). Average peri-event Z-score for dLight1.3b

signals in the NAc for day 1 (top row) and day 5 (middle row and bottom row) for (**E**) control (*N*=6), (**F**) Kv4.3 LOF (*N*=6), and (**G**) BKCa1.1 LOF (*N*=5) mice. (**H**) Average area under the curve (AUC) for the perievent Z-score dLight1.3b signals post-LP period (3 s) (*p<0.05; **p<0.01; ***p<0.001). (**I**) Average AUC for the Z-score for post-Rew period (5 s) (*p<0.05; ***p<0.001). (**J**) Average AUC for the Z-score for post- HE/CR period (5 s) (*p<0.05). (**K**) Average peak for pre-LP period (*p<0.05). (**L**) Average cumulative summation (CuSum) of the pre-LP period showing similar inflection (start of rise) but significant overall ramping activity in Kv4.3 LOF mice (***p<0.001).

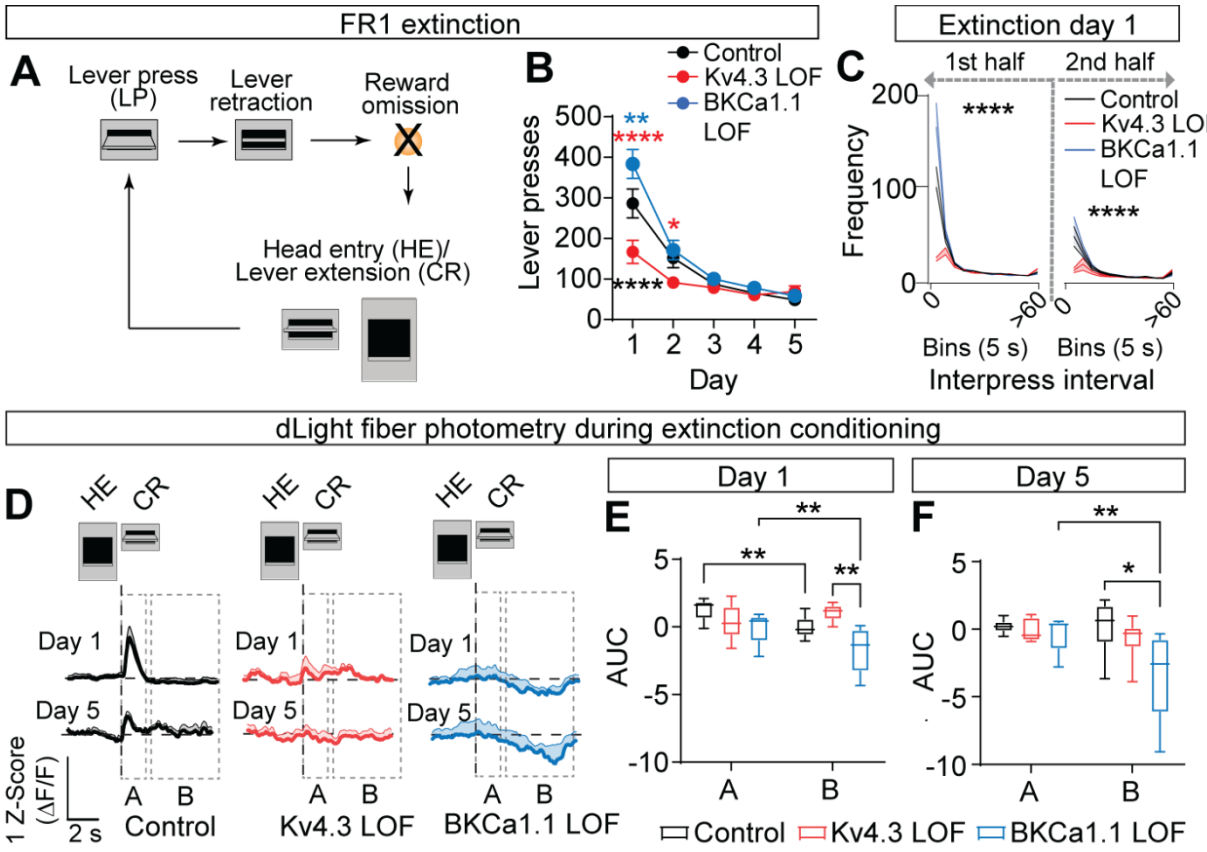

Fig. 4 Extinction behavior and dopamine signal changes in Kv4.3 and BKCa1.1 LOF mice.

(**A**) Schematic of instrumental FR1 extinction paradigm. (**B**) Lever presses during days 1-5 of extinction training ($N_{control}$=13, $N_{Kv4.3LOF}$=10, and $N_{BKCa1.1LOF}$=12; **p<0.01, blue= BKCa1.1 LOF vs. control; ****p<0.0001, red=BKCa1.1 LOF vs. Kv4.3 LOF; ****p<0.0001, black= Kv4.3 LOF vs. control). (**C**) Frequency distribution of lever presses during the first and second half of the conditioning session for day 1 of extinction (****P<0.0001). (**D**) Average Z-score for dLight1.3b signals in the NAc during HE/CR in control (*N*=6), KV4.3 LOF (*N*=6), and BKCa1.1 LOF (*N*=5) mice for day 1 and day 5. The signal was separated into the peri-HE/CR period (period A, 2 s) and the subsequent sustained 3 s period during omission (period B) for AUC analysis. (**E**) Average AUC for the Z-score for post-lever HE/CR during the A and B periods on day 1 (**p<0.01). (**E**)

Average AUC for the Z-score ΔF/F for post-lever HE/CR during the A and B periods on day 5 (*p<0.05; **p<0.01).